

Seebeck coefficient of underdoped $\text{La}_{2-x}\text{Sr}_x\text{CuO}_4$ in high magnetic fields : Fermi-surface reconstruction by charge-density-wave order

S. Badoux,^{1,*} S.A.A. Afshar,¹ B. Michon,¹ A. Ouellet,¹ S. Fortier,¹ D. LeBoeuf,² T.P. Croft,³ C. Lester,³ S.M. Hayden,³ H. Takagi,⁴ K. Yamada,⁵ D. Graf,⁶ N. Doiron-Leyraud,¹ and Louis Taillefer^{1,7,†}

¹*Département de physique & RQMP, Université de Sherbrooke, Sherbrooke, Québec J1K 2R1, Canada*

²*Laboratoire National des Champs Magnétiques Intenses,
UPR 3228, (CNRS-INSA-UJF-UPS), Grenoble 38042, France*

³*H. H. Wills Physics Laboratory, University of Bristol, Bristol, BS8 1TL, United Kingdom*

⁴*Department of Physics, University of Tokyo, Tokyo, Japan*

⁵*Institute of Materials Structure Science, High Energy Accelerator Research Organization
& The Graduate University for Advanced Studies, Oho, Tsukuba 305-0801, Japan*

⁶*National High Magnetic Field Laboratory, Tallahassee, FL 32310, USA*

⁷*Canadian Institute for Advanced Research, Toronto, Ontario M5G 1Z8, Canada*

(Dated: June 13, 2019)

The Seebeck coefficient S of the cuprate superconductor $\text{La}_{2-x}\text{Sr}_x\text{CuO}_4$ (LSCO) was measured in magnetic fields large enough to suppress superconductivity, for a range of Sr concentrations from $x = 0.07$ to $x = 0.15$. For $x = 0.11, 0.12, 0.125$ and 0.13 , S/T decreases upon cooling to become negative at low temperature. The same behavior is observed in the Hall coefficient $R_H(T)$. In analogy with other hole-doped cuprates at similar hole concentrations p , the negative S and R_H show that the Fermi surface of LSCO undergoes a reconstruction caused by the onset of charge-density-wave modulations. Such modulations have indeed been detected in LSCO by X-ray diffraction in precisely the same doping range. Our data show that in LSCO this Fermi-surface reconstruction is confined to $0.085 < p < 0.15$. We argue that in the field-induced normal state of LSCO, spin-density-wave order extends beyond $p = 0.15$ and it may thus be associated with the quantum critical behavior observed in the resistivity of LSCO around $p \simeq 0.2$.

Since the discovery of quantum oscillations [1] and a negative Hall coefficient R_H [2] in the cuprate superconductor $\text{YBa}_2\text{Cu}_3\text{O}_y$ (YBCO), it has become clear that the Fermi surface of underdoped YBCO undergoes a reconstruction at low temperature that produces a small electron pocket [3], in a doping range from $p = 0.08$ to $p \simeq 0.15$ [4]. This Fermi-surface reconstruction (FSR) was also detected as a sign change in the Seebeck coefficient $S(T)$, going from positive at high temperature to negative at low temperature [5]. A strikingly similar change of sign in $S(T)$ observed in the cuprate $\text{La}_{1.8-x}\text{Eu}_{0.2}\text{Sr}_x\text{CuO}_4$ (Eu-LSCO) [6] suggested that the stripe order known to exist in Eu-LSCO [7] – a combination of charge-density-wave (CDW) and spin-density-wave (SDW) modulations – is responsible for the FSR in both materials. The observation of CDW modulations in YBCO by NMR [8] and X-ray diffraction (XRD) [9, 10] confirmed this conjecture, and demonstrated that it is the CDW (and not the SDW) modulations that cause the FSR.

In YBCO, the drop in $R_H(T)$ and S/T begins at a temperature T_{max} that peaks at $p = 0.12$ (Fig. 1a). The drop is attributed to the CDW modulations detected by XRD [11, 12] and NMR [13] below a temperature T_{CDW} in the same doping range as the FSR [4], with T_{CDW} also peaking at $p = 0.12$ (Fig. 1a).

In $\text{HgBa}_2\text{CuO}_{4+\delta}$ (Hg1201), high-field measurements

of Hall and Seebeck coefficients revealed a similar FSR [14], confirmed by the observation of quantum oscillations [15] and again attributed to XRD-detected CDW modulations [16]. All this suggests that CDW modulations and the associated FSR are generic properties of hole-doped cuprates in the vicinity of $p = 0.12$. A major outstanding question is : Up to what critical doping p_{CDW} do CDW modulations extend in the phase diagram (Fig. 1), in particular in the field-induced normal state at $T = 0$? In this context, the material LSCO offers a powerful platform, since good crystals can be grown with p up to 0.3 and beyond. CDW modulations have been observed in LSCO with XRD, at $p \simeq 0.12$ [17–19], but there is little information about the associated FSR.

In this Article, we report high-field measurements of the Seebeck coefficient in LSCO single crystals at several dopings, which show that S becomes negative in the normal state at low temperature in precisely the doping range where CDW modulations are detected by XRD. R_H is also found to be negative in that range. The FSR in LSCO is therefore very similar to the FSR in YBCO and Hg1201. Our data show that the FSR does not extend above $p = 0.15$, strong evidence that CDW order in LSCO ends at a critical doping $p_{\text{CDW}} = 0.15$. Because SDW order is known to persist beyond $p = 0.15$ in the field-induced normal state [20–22], our findings reveal that CDW and SDW are not tied together into a single "stripe" state in LSCO, as indeed they are not tied in YBCO. It is then likely that the quantum criticality observed in the resistivity of LSCO around $p \simeq 0.2$ (ref. 23) is associated with "pure" SDW order.

* sven.badoux@usherbrooke.ca

† louis.taillefer@usherbrooke.ca

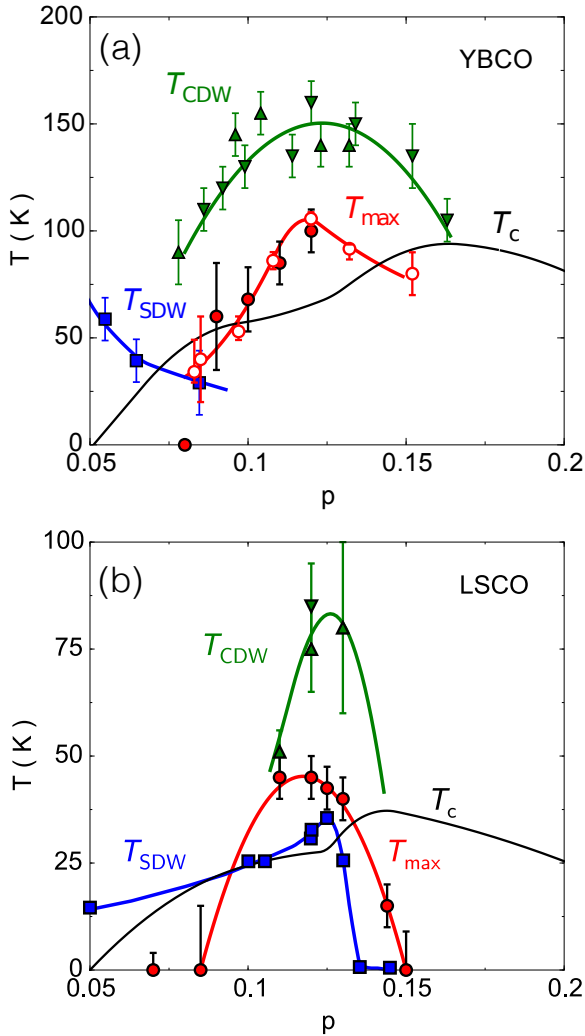


Figure 1. Temperature-doping phase diagram of the cuprate superconductors YBCO (a) and LSCO (b). The superconducting transition temperature T_c is drawn as a black line. Charge density-wave (CDW) modulations are detected by X-ray diffraction below T_{CDW} (green triangles) in YBCO (up triangles [11], down triangles [12]) and LSCO (up triangles [17], down triangle [19]). Spin-density-wave (SDW) modulations are detected by neutron diffraction below T_{SDW} (blue squares) in YBCO [24] and LSCO [21, 25–28]. When plotted as S/T vs T , the normal-state Seebeck coefficient peaks at a temperature T_{max} (full red circles) before it drops at low temperature due to Fermi-surface reconstruction (YBCO, ref. 6; LSCO, this work, Figs. 3 and 4). A similar T_{max} can also be defined for the Hall coefficient (open red circles), below which $R_H(T)$ drops at low temperature (YBCO, ref. 4).

Methods.— Single crystals of LSCO were grown by the flux-zone technique with Sr concentrations $x = 0.085$, 0.11, 0.12 and 0.13 at the University of Bristol, $x = 0.07$ and 0.125 at the University of Tokyo, $x = 0.144$ and 0.15 at Tohoku University. Samples were cut in the shape of rectangular platelets, with typical dimensions 0.5 mm \times 1.0 mm \times 0.1 mm. The hole concentration (doping) p is

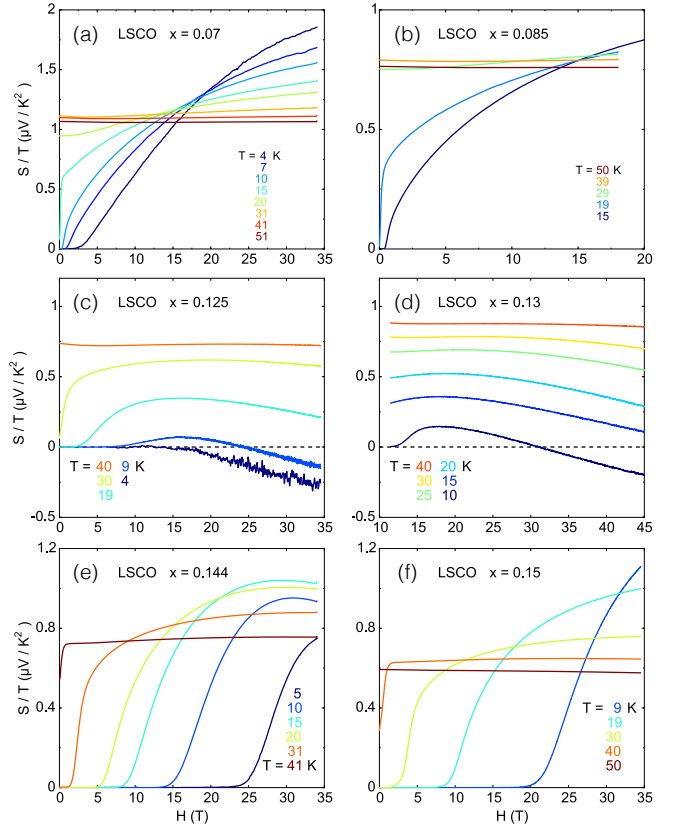


Figure 2. Isotherms of the Seebeck coefficient in LSCO, plotted as S/T vs magnetic field H , at various temperatures, as indicated, for six samples, with $x = 0.07$ (a), $x = 0.085$ (b), $x = 0.125$ (c), $x = 0.13$ (d), $x = 0.144$ (e), and $x = 0.15$ (f). For $x = 0.125$ and 0.13, S/T at high H decreases at low temperature, to reach negative values. For $x = 0.144$, S/T also decreases at low temperature, below 15 K. This decrease is the signature of FSR. In contrast, for $x = 0.07$ and 0.15, S/T at the highest measured field keeps increasing with decreasing temperature down to the lowest temperature. This shows that there is no FSR at those dopings, at least down to 4 K and 9 K, respectively. The same is true at $x = 0.085$, at least down to 15 K.

given by $p = x$. The (zero-resistance) superconducting transition temperature of the 8 samples is $T_c = 12.7, 20.2, 26.2, 27.5, 28.0, 32.3, 37.2,$ and 36.5 K for $p = 0.07, 0.085, 0.11, 0.12, 0.125, 0.13, 0.144,$ and 0.15 , respectively. The Seebeck coefficient was measured, as described elsewhere [6], at Sherbrooke (all samples) up to $H = 20$ T, at the NHMFL in Tallahassee up to $H = 34$ T ($x = 0.125$ and 0.15) and up to $H = 45$ T ($x = 0.13$), and at the LNCMI in Grenoble up to $H = 34$ T ($x = 0.07$ and 0.144). The Hall coefficient of samples with $x = 0.12, 0.125$ and 0.13 was measured, as described elsewhere [4], at Sherbrooke in $H = 16$ T. All crystals have an orthorhombic crystal structure and they are twinned. The thermal gradient or electrical current was applied in the basal plane, while the magnetic field was applied along the c axis.

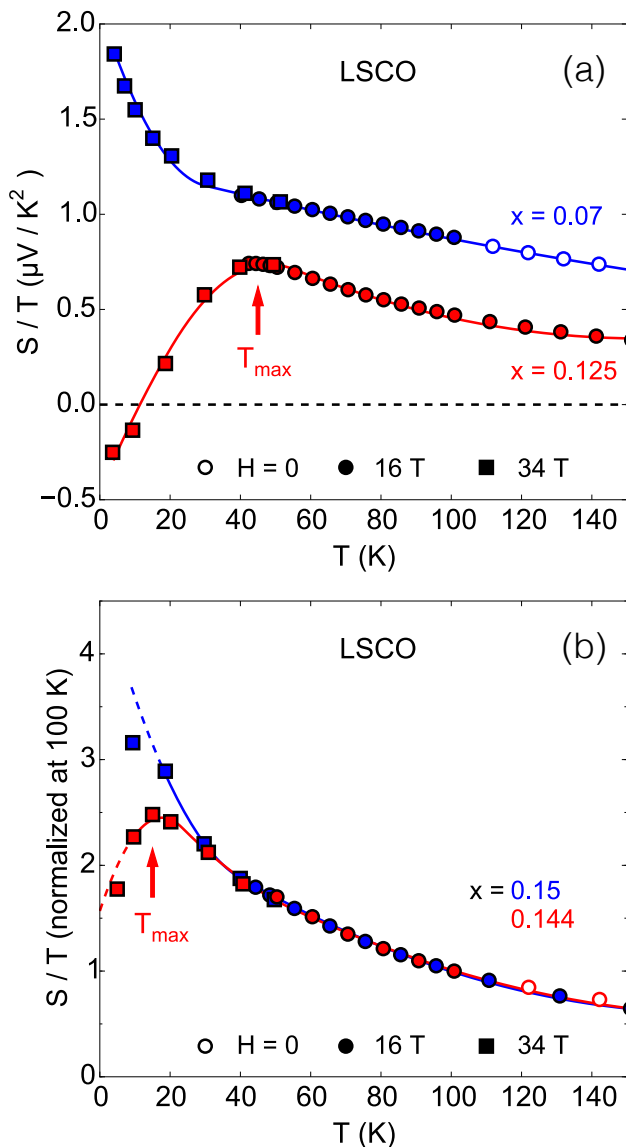


Figure 3. Seebeck coefficient of LSCO, plotted as S/T vs temperature T , measured in a magnetic field $H = 0$ (open circles), 16 T (full circles) and 34 T (squares), for four samples, with $x = 0.07$ and 0.125 (a), and $x = 0.144$ and 0.15 (b). The data in panel b are normalized to their value at $T = 100$ K. All data points represent the normal state, for which the solid lines are a guide to the eye, except the lowest point for each of $x = 0.144$ and $x = 0.15$ (panel b). For these two points, the isotherms are still going up the superconducting transition (Fig. 2). The dashed lines are an extension of the normal-state behavior based on extrapolating those isotherms beyond 34 T. T_{\max} marks the temperature below which S/T decreases at low temperature (arrow), in some cases to reach negative values, as seen here for $x = 0.125$. This decrease is the signature of Fermi-surface reconstruction (FSR). Note how the data for $x = 0.144$ and $x = 0.15$ diverge below $T \simeq 30$ K, with the former dropping at low T due to FSR and the latter showing no decrease, and hence no FSR (at least down to 9 K).

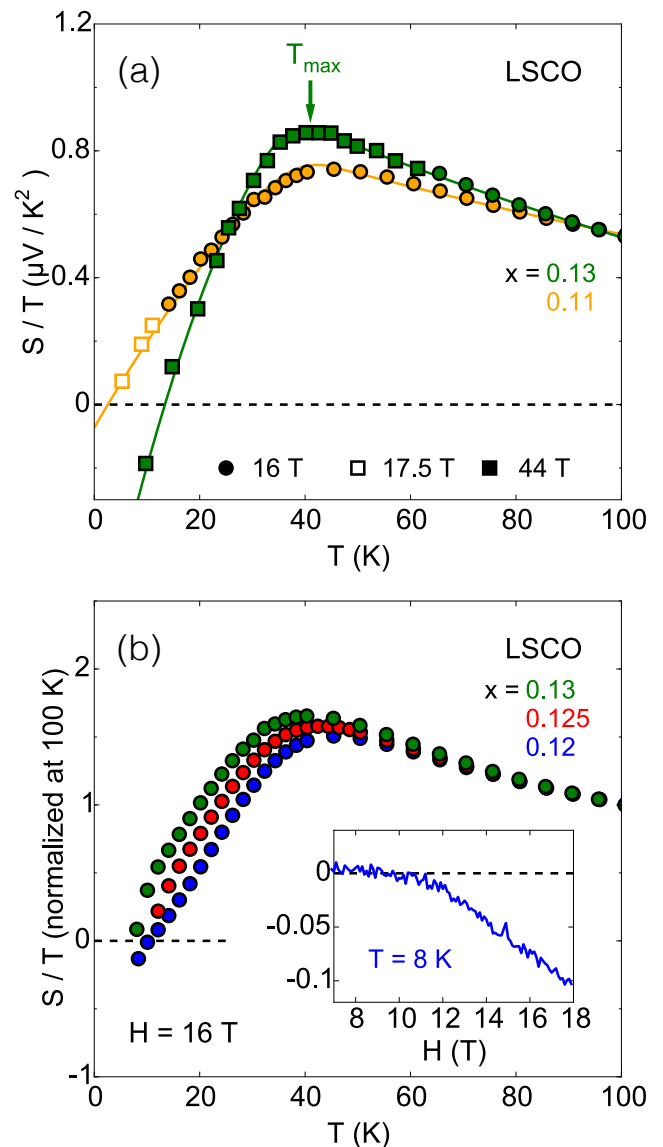


Figure 4. Same as in Fig. 3, for samples with $x = 0.11$ (yellow), $x = 0.12$ (blue), $x = 0.125$ (red) and $x = 0.13$ (green), measured at $H = 16$ T (full circles), 17.5 T (open squares) and 44 T (full squares). The data in panel b are normalized to their value at $T = 100$ K. FSR is clearly observed in all four samples, as a drop in S/T at low temperature. *Inset of panel b*: Isotherm at $T = 8$ K for $x = 0.12$, showing that S/T becomes increasingly negative with increasing field, demonstrating that the negative S is a property of the normal state.

Seebeck coefficient.— In Fig. 2, the Seebeck data for 6 samples are plotted as S/T vs H for several temperatures. We see that for $x = 0.125$ (Fig. 2c) and $x = 0.13$ (Fig. 2d), S becomes negative at high field and low temperature. This shows that a negative S is a property of the normal state of LSCO at these dopings, as in YBCO, Eu-LSCO and Hg1201. At $x = 0.144$, we see that at high field S/T decreases when the temperature drops be-

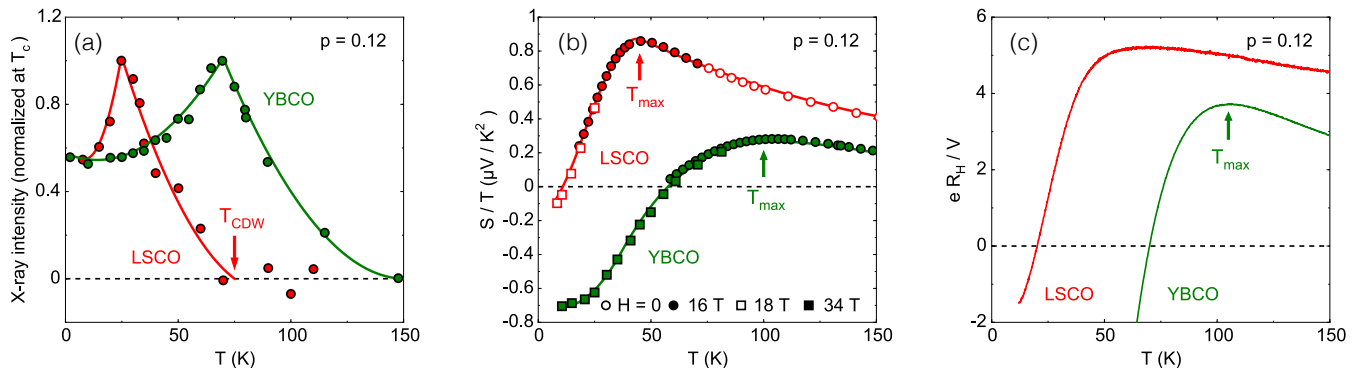


Figure 5. Comparison of LSCO (red) and YBCO (green) at $p = 0.12$. a) Temperature dependence of the X-ray intensity associated with the CDW modulations, normalized at T_c , detected in LSCO [17] and YBCO [10]. Lines are a guide to the eye. The cusp is at T_c . b) Normal-state Seebeck coefficient of LSCO (this work) and YBCO [6], measured in a magnetic field as indicated, plotted as S/T vs T . T_{max} is the temperature below which S/T drops to reach negative values at low temperature (arrow), the signature of Fermi-surface reconstruction (FSR). This T_{max} is plotted as full circles in Fig. 1. Lines are a guide to the eye. c) Hall coefficient of LSCO at $H = 16$ T and YBCO at $H = 15$ T [2], plotted as eR_H/V , where e is the electron charge and V the volume per planar Cu atom. T_{max} is the temperature below which $R_H(T)$ drops to reach negative values at low temperature (arrow), another signature of FSR. T_{max} is plotted as open circles in Fig. 1a [4].

low $T = 15$ K (Fig. 2e). In contrast, no such decrease is observed at $x = 0.15$, down to the lowest temperature (Fig. 2f). At $x = 0.07$, S/T increases steadily with decreasing T at high field, down to the lowest temperature (Fig. 2a). This is also true at $x = 0.085$ (Fig. 2b). Although here our data only goes to 20 T, the crossing of the lowest isotherms shows that S/T keeps increasing down to $T = 15$ K, at least.

In Figs. 3 and 4, we plot S/T vs T , at high field. In Fig. 3a, we see that the drop in S/T at $x = 0.125$ to negative values starts below a temperature $T_{max} \simeq 40$ K. This is also the case at $x = 0.11$ and 0.13 (Fig. 4a). In Fig. 4b, we compare data on 3 samples taken in identical conditions, at $H = 16$ T. (Although the LSCO sample with $x = 0.12$ was only measured up to 18 T, S/T at $T = 8$ K is increasingly negative with increasing H (inset of Fig. 4b), confirming that a negative S is a property of the normal state also at that doping.) The location of the peak in S/T vs T is seen to decrease from $T_{max} = 45$ K at $x = 0.12$, to $T_{max} = 42.5$ K at $x = 0.125$, to $T_{max} = 40$ K at $x = 0.13$. Those T_{max} values are plotted on the phase diagram of LSCO in Fig. 1b. Raising the doping further, we observe that T_{max} continues its steady descent. Indeed, at $p = 0.144$, S/T now peaks at $T_{max} \simeq 15$ K (Fig. 3b). Extrapolating this trend yields $T_{max} \rightarrow 0$ at $p \rightarrow 0.15$ (Fig. 1a). Our data at $x = 0.15$ confirm this, with S/T showing no decrease down to at least 9 K (Figs. 2f and 3b). This shows that FSR in LSCO ends at a critical doping $p_{FSR} = 0.15 \pm 0.005$.

At $x = 0.07$, the normal-state S/T increases monotonically with decreasing T , down to our lowest temperature (Fig. 3a). There is clearly no FSR at that doping. At $x = 0.085$, although we only measured up to 18 or 20 T, we observe that S/T at $H = 18$ T increases as $T \rightarrow 0$, at least down to 15 K (Fig. 2b). So here $T_{max} < 15$ K. In

Fig. 1b, we plot T_{max} vs p for our 8 samples, with their uncertainty, and thereby delineate the region where FSR occurs in the $T - p$ phase diagram of LSCO. We see that the FSR region peaks at $p \simeq 0.12$ and is confined between $p \simeq 0.085$ and $p = p_{FSR} = 0.15 \pm 0.005$.

Hall coefficient.— In Fig. 5c, the Hall coefficient of our LSCO crystal with $x = 0.12$, measured at $H = 16$ T, is plotted as R_H vs T . We see that $R_H(T)$ drops below $T \simeq 50$ K and becomes negative below $T \simeq 20$ K. Data for our crystals with $x = 0.125$ and $x = 0.13$ are very similar, also negative at low T , all in excellent agreement with prior low-field data on single crystals of LSCO with $x = 0.12$ [29]. (The absence of a negative R_H in previous high-field data on thin films of LSCO [30] may be due to the higher disorder of such samples.) A similar drop in $R_H(T)$ has been seen in Eu-LSCO [31] and in $\text{La}_{1.4-x}\text{Nd}_{0.6}\text{Sr}_x\text{CuO}_4$ (Nd-LSCO) [32], when $p \simeq 0.12$; in both materials, it is closely linked to the onset of CDW order.

Discussion.— Taken together, the negative Hall and Seebeck coefficients in the normal state of LSCO are conclusive evidence of FSR in this material, in the vicinity of $p = 0.12$. This adds to the previous three cases, namely YBCO, Eu-LSCO and Hg1201. In all 4 cases, the FSR occurs in a region of the $T - p$ phase diagram where CDW modulations have been detected by XRD (Fig. 1). The link between CDW and FSR is robust.

It is instructive to compare LSCO and YBCO. The two phase diagrams are similar (Fig. 1). In both cases, T_{max} and T_{CDW} peak at $p = 0.12$, and the region of FSR is confined to similar ranges – from $p \simeq 0.085$ to $p = 0.15$ in LSCO and from $p = 0.08$ to $p \simeq 0.15$ in YBCO [4]. In Fig. 5, we compare data for LSCO and YBCO directly,

at $p = 0.12$. The CDW modulations detected by XRD emerge below a temperature twice as high in YBCO compared to LSCO (Fig. 5a) : $T_{\text{CDW}} \simeq 150$ K in YBCO vs $T_{\text{CDW}} \simeq 75$ K in LSCO. Correspondingly, the FSR is detected at a temperature twice as high in YBCO compared to LSCO, with $T_{\text{max}} \simeq 100$ K in YBCO vs $T_{\text{max}} \simeq 50$ K in LSCO (Fig. 5b). All this suggests that CDW ordering is a stronger tendency in YBCO than in LSCO. Intriguingly, the superconducting transition temperature T_c is roughly twice as high in YBCO as compared to LSCO (see cusp in Fig. 5a). This raises the interesting possibility that the same underlying mechanism, perhaps magnetic, fuels both superconductivity and CDW order [33].

Given that FSR in LSCO ends at $p_{\text{FSR}} = 0.15$, we infer that this is also where CDW order ends. This is consistent with recent XRD measurements that detect no CDW modulations in LSCO at $x = 0.15$ [34]. (The same consistency is observed at $x = 0.085$, where again no CDW modulations are detected by XRD [34].) We thus arrive at a key information : the CDW phase in LSCO ends at the critical doping $p_{\text{CDW}} = 0.15$.

Neutron diffraction studies show that SDW order exists in LSCO at low temperature up to $p \simeq 0.13$, in zero magnetic field [21, 25] (Fig. 1b) suggesting the presence of a quantum critical point. This is supported by the observation of diverging spin fluctuations as $T \rightarrow 0$ for $p \simeq 0.14$ [35]. As theoretically expected for competing SDW and superconducting phases [36], application of a magnetic field (along the c axis) pushes this critical doping upwards, such that 7 T is enough to induce SDW order at $p = 0.145$ [20–22]. Extrapolating the boundary of the SDW phase in the $H - p$ plane indicates that SDW order in LSCO could extend up to $p = p_{\text{SDW}} \simeq 0.2$ when $H > 50$ T [21]. It is then likely that the perfectly linear temperature dependence of the resistivity as $T \rightarrow 0$ observed in LSCO at $p \simeq 0.2$

[23] is associated with SDW quantum criticality. Given that the linear- T resistivity is a universal property of cuprates [37], such a quantum critical point would then be a universal feature of cuprate superconductors.

Summary.— Our high-field measurements of the Seebeck coefficient in the cuprate superconductor LSCO reveal that its normal-state Fermi surface undergoes a reconstruction at low temperature, in the doping range $0.085 < p < 0.15$. In analogy with the cuprates YBCO, Eu-LSCO and Hg1201, we attribute this FSR to the CDW modulations detected by XRD in the very same doping range. Combined with XRD data on LSCO, our Seebeck data make a compelling case that CDW modulations disappear at $p = p_{\text{CDW}} = 0.15$, so that the field-induced non-superconducting ground state of LSCO above $p = 0.15$ is one with SDW order alone. This shows that SDW order can exist independently of CDW order in LSCO. We propose that the quantum critical point where this SDW order ends, at $p = p_{\text{SDW}} \simeq 0.2$, could account for the linear- T resistivity at $T \rightarrow 0$ observed at that doping.

Acknowledgements.— A portion of this work was performed at the National High Magnetic Field Laboratory, which is supported by the National Science Foundation Cooperative Agreement No. DMR- 1157490, the State of Florida, and the U.S. Department of Energy. Another portion of this work was performed at the Laboratoire National des Champs Magnétiques Intenses of the CNRS, member of the European Magnetic Field Laboratory. L.T. acknowledges support from the Canadian Institute for Advanced Research (CIFAR) and funding from the National Science and Engineering Research Council of Canada (NSERC), the Fonds de recherche du Québec - Nature et Technologies (FRQNT), the Canada Foundation for Innovation (CFI) and a Canada Research Chair.

-
- [1] N. Doiron-Leyraud, C. Proust, D. LeBoeuf, J. Levallois, J-B. Bonnemaïson, R. Liang, D. A. Bonn, W. N. Hardy, and L. Taillefer, *Nature* **447**, 565 (2007).
 - [2] D. LeBoeuf, N. Doiron-Leyraud, J. Levallois, R. Daou, J-B. Bonnemaïson, N. E. Hussey, L. Balicas, B. J. Ramshaw, R. Liang, D. A. Bonn, W. N. Hardy, S. Adachi, C. Proust, and L. Taillefer, *Nature* **450**, 533 (2007).
 - [3] L. Taillefer, *J. Phys.: Condens. Matter* **21**, 164212 (2009).
 - [4] D. LeBoeuf, N. Doiron-Leyraud, B. Vignolle, M. Sutherland, B. J. Ramshaw, J. Levallois, R. Daou, F. Laliberté, O. Cyr-Choinière, J. Chang, Y. J. Jo, L. Balicas, R. Liang, D. A. Bonn, W. N. Hardy, C. Proust, and L. Taillefer, *Phys. Rev. B* **83**, 054506 (2011).
 - [5] J. Chang, R. Daou, C. Proust, D. LeBoeuf, N. Doiron-Leyraud, F. Laliberté, B. Pingault, B. J. Ramshaw, R. Liang, D. A. Bonn, W. N. Hardy, H. Takagi, A. B. Antunes, I. Sheikin, K. Behnia, and L. Taillefer, *Phys. Rev. Lett.* **104**, 057005 (2010).
 - [6] F. Laliberté, J. Chang, N. Doiron-Leyraud, E. Hassinger, R. Daou, M. Rondeau, B.J. Ramshaw, R. Liang, D. A. Bonn, W. N. Hardy, S. Pyon, T. Takayama, H. Takagi, I. Sheikin, L. Malone, C. Proust, K. Behnia, and L. Taillefer, *Nat. Commun.* **2**, 432 (2011).
 - [7] J. Fink, V. Soltwisch, J. Geck, E. Schierle, E. Weschke, and B. Buchner, *Phys. Rev. B* **83**, 092503 (2011).
 - [8] T. Wu, H. Mayaffre, S. Krämer, M. Horvatić, C. Berthier, W. N. Hardy, R. Liang, D. A. Bonn, and M-H. Julien, *Nature* **477**, 191 (2011).
 - [9] G. Ghiringhelli, M. Le Tacon, M. Minola, S. Blanco-Canosa, C. Mazzoli, N. B. Brookes, G. M. De Luca, A. Frano, D. G. Hawthorn, F. He, T. Loew, M. Moretti Sala, D. C. Peets, M. Salluzzo, E. Schierle, R. Sutarto, G. A. Sawatzky, E. Weschke, B. Keimer, and L. Braicovich, *Science* **337**, 821 (2012).
 - [10] J. Chang, E. Blackburn, A. T. Holmes, N. B. Christensen, J. Larsen, J. Mesot, R. Liang, D. A. Bonn, W. N. Hardy, A. Watenphul, M. v Zimmermann, E. M. Forgan,

- and S. M. Hayden, *Nat. Phys.* **8**, 871 (2012).
- [11] M. Hücker, N. B. Christensen, A. T. Holmes, E. Blackburn, E. M. Forgan, R. Liang, D. A. Bonn, W. N. Hardy, O. Gutowski, M. v. Zimmermann, S. M. Hayden, and J. Chang, *Phys. Rev. B* **90**, 054514 (2014).
- [12] S. Blanco-Canosa, A. Frano, E. Schierle, J. Porras, T. Loew, M. Minola, M. Bluschke, E. Weschke, B. Keimer, and M. Le Tacon, *Phys. Rev. B* **90**, 054513 (2014).
- [13] T. Wu, H. Mayaffre, S. Krämer, M. Horvatić, C. Berthier, W. N. Hardy, R. Liang, D. A. Bonn, and M.-H. Julien, *Nat. Commun.* **6**, 6438 (2015).
- [14] N. Doiron-Leyraud, S. Lepault, O. Cyr-Choinière, B. Vignolle, G. Grissonnanche, F. Laliberté, J. Chang, N. Barišić, M. K. Chan, L. Ji, X. Zhao, Y. Li, M. Greven, C. Proust, and L. Taillefer, *Phys. Rev. X* **3**, 021019 (2013).
- [15] N. Barišić, S. Badoux, M. K. Chan, C. Dorow, W. Tabis, B. Vignolle, G. Yu, J. Béard, X. Zhao, C. Proust, and M. Greven, *Nat. Phys.* **9**, 761 (2013).
- [16] W. Tabis, Y. Li, M. Le Tacon, L. Braicovich, A. Kreyssig, M. Minola, G. Della, E. Weschke, M. J. Veit, M. Ramazanoglu, A. I. Goldman, T. Schmitt, G. Ghiringhelli, N. Barišić, M. K. Chan, C. J. Dorow, G. Yu, X. Zhao, B. Keimer, and M. Greven, *Nat. Commun.* **5**, 5875 (2014).
- [17] T. P. Croft, C. Lester, M. S. Senn, A. Bombardi, and S. M. Hayden, *Phys. Rev. B* **89**, 224513 (2014).
- [18] V. Thampy, M. P. M. Dean, N. B. Christensen, L. Steinke, Z. Islam, M. Oda, M. Ido, N. Momono, S. B. Wilkins, and J. P. Hill, *Phys. Rev. B* **90**, 100510 (2014).
- [19] N. B. Christensen, J. Chang, J. Larsen, M. Fujita, M. Oda, M. Ido, N. Momono, E. M. Forgan, A. T. Holmes, J. Mesot, M. Huecker, and M. v Zimmermann, *arXiv:1404.3192* (2014).
- [20] B. Khaykovich, S. Wakimoto, R. J. Birgeneau, M. A. Kastner, Y. S. Lee, P. Smeibidl, P. Vorderwisch, and K. Yamada, *Phys. Rev. B* **71**, 220508 (2005).
- [21] J. Chang, Ch. Niedermayer, R. Gilardi, N. B. Christensen, H. M. Ronnow, D. F. McMorrow, M. Ay, J. Stahn, O. Sobolev, A. Hiess, S. Pailhes, C. Baines, N. Momono, M. Oda, M. Ido, and J. Mesot, *Phys. Rev. B* **78**, 104525 (2008).
- [22] J. Chang, N. B. Christensen, C. Niedermayer, K. Lefmann, H. M. Ronnow, D. F. McMorrow, A. Schneidewind, P. Link, A. Hiess, M. Boehm, R. Mottl, S. Pailhes, N. Momono, M. Oda, M. Ido, and J. Mesot, *Phys. Rev. Lett.* **102**, 177006 (2009).
- [23] R. A. Cooper, Y. Wang, B. Vignolle, O. J. Lipscombe, S. M. Hayden, Y. Tanabe, T. Adachi, Y. Koike, M. Nohara, H. Takagi, C. Proust, and N. E. Hussey, *Science* **323**, 603 (2009).
- [24] D. Haug, V. Hinkov, Y. Sidis, P. Bourges, N. B. Christensen, A. Ivanov, T. Keller, C. T. Lin, and B. Keimer, *New J. Phys.* **12**, 105006 (2010).
- [25] M. Kofu, S.-H. Lee, M. Fujita, H.-J. Kang, H. Eisaki, and K. Yamada, *Phys. Rev. Lett.* **102**, 047001 (2009).
- [26] S. Wakimoto, G. Shirane, Y. Endoh, K. Hirota, S. Ueki, K. Yamada, R. J. Birgeneau, M. A. Kastner, Y. S. Lee, P. M. Gehring, and S. H. Lee, *Phys. Rev. B* **60**, R769 (1999).
- [27] B. Lake, H. M. Rønnow, N. B. Christensen, G. Aeppli, K. Lefmann, D. F. McMorrow, P. Vorderwisch, P. Smeibidl, N. Mangkorntong, T. Sasagawa, M. Nohara, H. Takagi, and T. E. Mason, *Nature* **415**, 299 (2002).
- [28] H. Kimura, K. Hirota, H. Matsushita, K. Yamada, Y. Endoh, S.-H. Lee, C. F. Majkrzak, R. Erwin, G. Shirane, M. Greven, Y. S. Lee, M. A. Kastner, and R. J. Birgeneau, *Phys. Rev. B* **59**, 6517 (1999).
- [29] T. Suzuki, T. Goto, K. Chiba, M. Minami, Y. Oshima, T. Fukase, M. Fujita, and K. Yamada, *Phys. Rev. B* **66**, 104528 (2002).
- [30] F. F. Balakirev, J. B. Betts, A. Migliori, I. Tsukada, Y. Ando, and G. S. Boebinger, *Phys. Rev. Lett.* **102**, 017004 (2009).
- [31] O. Cyr-Choinière, R. Daou, F. Laliberté, D. LeBoeuf, N. Doiron-Leyraud, J. Chang, J.-Q. Yan, J.-G. Cheng, J.-S. Zhou, J. B. Goodenough, S. Pyon, T. Takayama, H. Takagi, Y. Tanaka, and L. Taillefer, *Nature* **458**, 743 (2009).
- [32] T. Noda, H. Eisaki, and S. Uchida, *Science* **286**, 265 (1999).
- [33] K. B. Efetov, H. Meier, and C. Pépin, *Nat. Phys.* **9**, 442 (2013).
- [34] T. P. Croft and S. M. Hayden, private communication.
- [35] G. Aeppli, T. E. Mason, S. M. Hayden, H. A. Mook, and J. Kulda, *Science* **278**, 1432 (1997).
- [36] E. Demler, S. Sachdev, and Y. Zhang, *Phys. Rev. Lett.* **87**, 067202 (2001).
- [37] L. Taillefer, *Annu. Rev. Condens. Matter Phys.* **1**, 51 (2010).